Chinese Chemical Letters 30 (2019) 949–952

Contents lists available at ScienceDirect

Chinese Chemical Letters

journal homepage: www.elsevier.com/locate/cclet

Communication

A multi-color and white-light emissive cucurbituril/terpyridine/lanthanide supramolecular nanofiber

Ting Zhang[a,b], Yaohua Liu[b], Bowen Hu[a,**], Chunhua Zhang[a], Yong Chen[b,c], Yu Liu[b,c,*]

[a] MIIT Key Laboratory of Critical Materials Technology for New Energy Conversion and Storage, School of Chemistry and Chemical Engineering, Harbin Institute of Technology, Harbin 150001, China
[b] College of Chemistry, State Key Laboratory of Elemento-Organic Chemistry, Nankai University, Tianjin 300071, China
[c] Collaborative Innovation Center of Chemical Science and Engineering (Tianjin), Tianjin 300072, China

ARTICLE INFO

Article history:
Received 2 November 2018
Received in revised form 5 December 2018
Accepted 27 December 2018
Available online 27 December 2018

Keywords:
Lanthanide luminescence
Cucurbit[8]uril
Host-guest interaction
White-light emission
Supramolecular chemistry

ABSTRACT

Multi-color and white light luminescence materials based on supramolecular assemblies are attractive because of their potential applications in advanced light-emitting material. Herein, a cucurbit[8]uril-enhanced lanthanide luminescent supramolecular assembly was constructed in a facile but efficient way using terpyridine imidozalium cations, cucurbit[8]urils and rare earth ions such as Tb^{3+} and Eu^{3+}. Significantly, the resultant fibrous supramolecular assembly, with an average width of 15 nm, could emit remarkable lanthanide luminescence, which was ten times higher than the corresponding terpyridine/Ln^{3+} without cucurbit[8]uril. And the solid state luminescence of supramolecular assembly could be smartly and easily turned among blue, green, red and white by adjusting the molar ratios between Tb^{3+} and Eu^{3+}. The enhanced white-light emission by supramolecular strategy may provide a new approach for smart and tunable solid luminescent materials.

Rare earth luminescence materials have recently emerged as a powerful strategy in the design of various types of advanced functional materials [1–4]. Lanthanide ions are ideal luminescence emitters because of their superior optical properties, such as sharp and stable emission peaks, long lifetime, intense luminescence, and resistance to photobleaching [5]. Among these, luminescent materials based on supramolecular assemblies are attractive because the host-guest complexation is an effective way for inducing, enhancing and adjusting various optical properties such as UV-vis absorbance, fluorescence, and circular dichroism [6–8]. Integrating dynamic metal-ligand coordination with supramolecular assemblies, a simple mixing approach offers remarkable versatility in the design of multi-stimuli-responsive luminescence materials [9]. In this method, well-ordered architectures bearing novel photophysical properties are formed spontaneously from individual chromophore components by non-covalent interactions such as hydrophobic interactions, π-π stacking, H-bonding, and charge transfer interactions. Recently, we reported the fluorescence-tunable supramolecular hydrogels especially emitting white-light achieved by swelling hydrogels in solutions containing two kinds of dyes [10].

Cucurbit[n]urils, cyclodextrins, crown ethers, cryptands and calixarenes all played a crucial role in supramolecular chemistry and materials science in recent decades [11–16]. Among these, possessing higher binding affinity, cucurbit[n]urils (CBs) is attributable to their shape (narrow portals and wide hydrophobic cavity) and the carbonyl groups, which provides selective binding towards positively charged guest molecules. In addition, high binding affinity and selectivity, recognition properties and good water-solubility of cucurbit[8]urils (CB[8]) make it widely useful in biological, photochemical, electrochemical, catalytic and optoelectronic applications [17–28]. In the previous studies, numerous supramolecular assemblies have been successfully fabricated *via* CB[8]-assisted host-guest interactions. For example, Scherman *et al.* reported a variety of supramolecular polymer networks, consisting of guest-pendant copolymers and CB[8] host molecules, which exploited the dynamic crosslinking of guest moieties through CB[8]-mediated host-guest ternary complexations [29]. Masson *et al.* showed that Fe(II) and Ir(III) bisterpyridine complexes underwent social self-sorting in the presence of CB[8] and assembled to dynamic oligomers with alternating Fe and Ir metallic cores [30,31]. However, little work about luminescence property combining dynamic metal-ligand coordination and cucurbituril-based supramolecular assembly were reported.

* Corresponding author at: College of Chemistry, State Key Laboratory of Elemento-Organic Chemistry, Nankai University, Tianjin 300071, China.
** Corresponding author.
E-mail addresses: bowenhu@hit.edu.cn (B. Hu), yuliu@nankai.edu.cn (Y. Liu).

https://doi.org/10.1016/j.cclet.2018.12.029
1001-8417/

Herein, we wish to report an enhanced and stable solid-state luminescence of fibrous supramolecular assembly based cucurbit[8]uril and a terpyridine derivative (TpyM) coordinated with Ln$(NO_3)_3{\cdot}6H_2O$. The terpyridine (tpy) group is an excellent sensitizer for lanthanide ions [32,33], so introducing Tpy groups as chelating ligands to coordinate with Tb^{3+} or Eu^{3+} resulted in TpyM-Tb^{3+} or TpyM-Eu^{3+} complex which showed green or red emission. Significantly, by adjusting the Tb^{3+}:Eu^{3+} ratio of CB[8]/TpyM-Ln^{3+} supramolecular assembly led to an efficient and tunable multi-color fluorescence emission varying among green, cyan, white, orange and red (Scheme 1). The enhanced solid-state luminescence, especially the white-light emission, *via* the formation of fibrous polymetallic supramolecular assembly would enable the potential application of cucurbituril-mediated supramolecular systems in smart light-emitting materials.

The cationic guest TpyM was prepared in 84% yield by the reaction of 4'-(4-(bromomethyl)phenyl)-2,2':6',2''-terpyridine (**2**) with 1-methylimidazole, and the reference compounds 4'-(*p*-tolyl)-2,2':6',2''-terpyridine (**1**) was prepared in 63% yield. It is well-known that lanthanide ions are emissive with high color purity, due to their narrow emission bands and the core nature of 4f orbitals, which could be shielded from the ligand environment by the filled 5s and 5p orbitals [34–36]. The long luminescence lifetimes of Ln^{3+} ions are a result of the parity forbidden nature of f-f transitions [37], leading to the inefficient direct excitation of metal ion-centered emission. Thus organic ligands are often used as optical antennae or sensitizers to transfer energy to the emissive excited states of Ln^{3+}. Herein, the terpyridine (Tpy) group was selected as an "antenna" for Ln^{3+}. Job analysis by UV-vis spectroscopy (Fig. S8 in Supporting information) gave the stoichiometric 2:1 binding ratio between TpyM and Ln^{3+}. In addition, ^{1}H NMR spectra showed that, after the addition of 0.5 equiv. of $Tb(NO_3)_3{\cdot}6H_2O$, the aromatic protons of Tpy moiety in TpyM presented both upfield and downfield shifts, accompanied by the obvious passivation (Fig. S7 in Supporting information). These results together demonstrate that Ln^{3+} was chelated with TpyM to form a stable metal complex.

Then, CB[8] was further introduced to form a supramolecular assembly system with TpyM-Ln^{3+} through the association of methylimidazole cation with CB[8] cavity.

The zeta potential ascended from + 1.63 mV (compound **2**) to + 13.75 mV (TpyM) proved the successful modification of imizolium-onium salt (Supporting information, the absorption maximum of CB[8]/TpyM-Tb^{3+}/Eu^{3+} exhibited the apparent bathochromic shift by 6 nm (from 275 nm to 281 nm) and a new absorption emerged at 341 nm upon continuous addition of equivalent CB[8], probably originated from the intermolecular charge-transfer(CT) interaction. ^{1}H NMR spectra of TpyM-Ln^{3+} and CB[8]/TpyM-Ln^{3+} showed that all the proton signals assigned to TpyM-Ln^{3+} underwent an obvious downfield shift and a broadened pattern upon addition of CB[8], and the proton signals of H_f and H_g displayed a upfield shift, indicating that two reference molecules were concurrently located in the CB[8] cavity to form CB[8]/TpyM-Ln^{3+} complex. In addition, the zeta potential of CB[8]/TpyM-Ln^{3+} at different hours for 3 days were shown in Figs. S6c and S6d. The zeta potential did not change obviously, which proved the good stability of the nanofibers.

The binding stoichiometry of TpyM-Ln^{3+} with CB[8] was further verified by a Job plot, where a maximum peak at a molar ratio of 0.5 was observed. This indicated a 1:1 host guest binding stoichiometry (Figs. S10b and S10d). The association constants (K_a) could be calculated as 4.65×10^6 L/mol and 3.25×10^6 L/mol, using a nonlinear least-squares curve-fitting method by analyzing the sequential changes in the UV-vis absorbance of TpyM-Tb^{3+} and TpyM-Eu^{3+} in the presence of varying concentrations of CB[8].

Transmission electron microscopy (TEM) and scanning electron microscopy (SEM) also supported the host-guest molecular assembly behavior of CB[8] with TpyM-Ln^{3+}. Without CB[8], TpyM-Tb^{3+} or TpyM-Eu^{3+} complex formed stable spherical nanoparticles (Fig. 2c) with an average diameter of *ca.* 60 nm in TEM images. When CB[8] was added, the nanoparticles disappeared, and new wire-like nanofibers with a length of hundreds of nanometers and a width of 15 nm were observed. In the control experiment, by using CB[7] with smaller cavity, there is only one guest encapsulated in it. The ^{1}H NMR signals of protons H a-e displayed a dramatic upfield shift, while those of protons H f–l in TpyM-Ln^{3+} showed a slight downfield shift, indicating that the

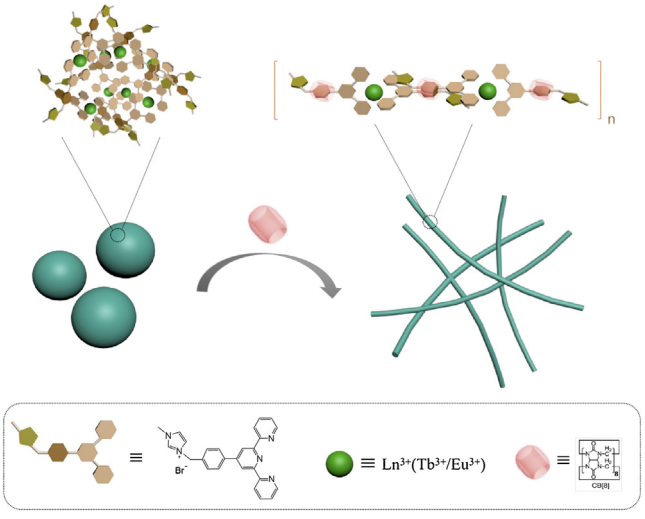

Scheme 1. Schematic illustration of the tunable ultra-strong lanthanide luminescence in solid by cucurbit[8]uril-based host-guest.

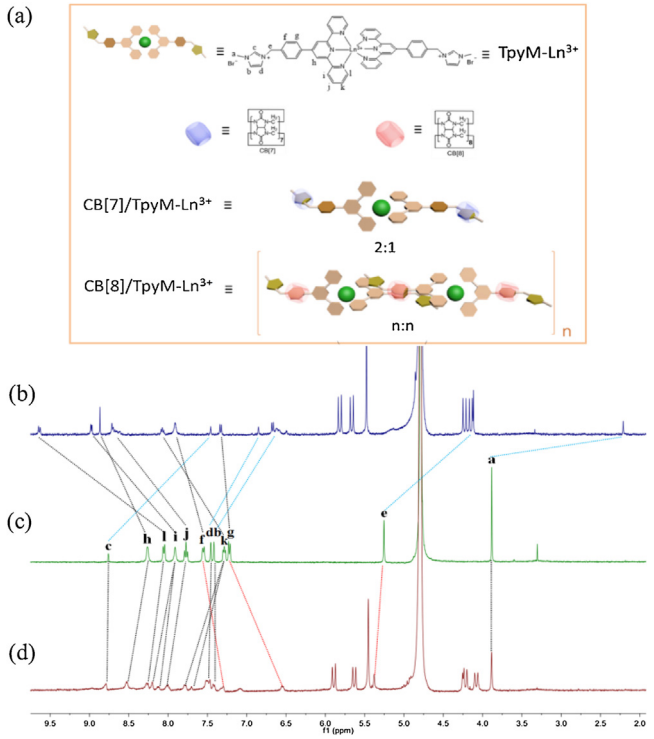

Fig. 1. (a) Schematic illustration of TpyM-Ln^{3+}, and the formation of CB[7]/TpyM-Ln^{3+} and wire-like supramolecular assembly CB[8]/TpyM-Ln^{3+}. ^{1}H NMR spectra monitoring the host-guest interaction of (b) CB[7]/TpyM-Ln^{3+} (2:1), (c) TpyM-Ln^{3+}, (d) CB[8]/TpyM-Ln^{3+} (n:n) (Ln = Tb).

imidazole segment was associated with CB[7] (Fig. 1b). The Job plot of TpyM-Ln^{3+} gave a maximum peak at a molar ratio of 0.66 referring to a 2:1 host-guest binding stoichiometry (Figs. S10a and S10c), indicating that one CB[7] cavity could only associate one methylimidazole moiety of TpyM-Ln^{3+}. Importantly, no wire-like supramolecular assembly could be observed in the TEM or SEM images of CB[7]/TpyM-Ln^{3+} system. Therefore, in the presence of CB[8]s as linkers, the 1:2 binding of one CB[8] with two adjacent TpyM-Ln^{3+} units to construct a linear supramolecular assembly, as illustrated in Fig. 1a, which could be the reason for the morphological change from nanoparticles to nanowires. Similar fibrous structures were also observed in SEM images (Fig. 2h). Considering the average width (15 nm measured by TEM) of nanofibers, a possible secondary aggregation of several CB[8]/TpyM-Ln^{3+} assemblies along the perpendicular direction of nanowires should not be ruled out.

Interestingly, a CB[8]-induced enhancement of solid fluorescence emission of CB[8]/TpyM-Ln^{3+} assembly was observed. As shown in Fig. 3, CB[8]/TpyM-Ln^{3+} emitted the strong blue, green and red fluorescences when excited at 254 nm. The enhanced fluorescence may be caused by two factors: (1) CB[8], a unique macrocycle with a rigid symmetrical structure and high binding affinity, is able to form stable complexes with cationic molecules. Once a certain amount of CB[8] was added to TpyM-Ln^{3+}, the formation of wire-like supramolecular assembly lead to the reduction of molecule vibration and the decrease of collision with other molecules, then the increase of fluorescence intensity. (2) The Typ group is an excellent sensitizer for lanthanide ions. The chelating ligand can absorb energy and generate a singlet (^{1}S) excited state. With the heavy atom effect, the ^{1}S state underwent intersystem crossing to populate an excited triplet (^{3}T) state, and then transferred energy from ligand to Ln^{3+}. The guest possessed a Typ group and a positive imidazonium (electron-drawing) group, while the CB[8] as an electron-donating group may lead to the energy more compatible with Ln^{3+}. Therefore, the supramolecular assembly produced stronger lanthanide luminescence. In addition, the binding effect of CB[8] changed the electron transition properties of TpyM and TpyM-Ln^{3+} with the red shift of absorption (Fig. S9). Meanwhile, the photos (irradiate by 254 nm UV light) of solid luminescence of CB[8]/TpyM-Ln^{3+} showed a great improvement

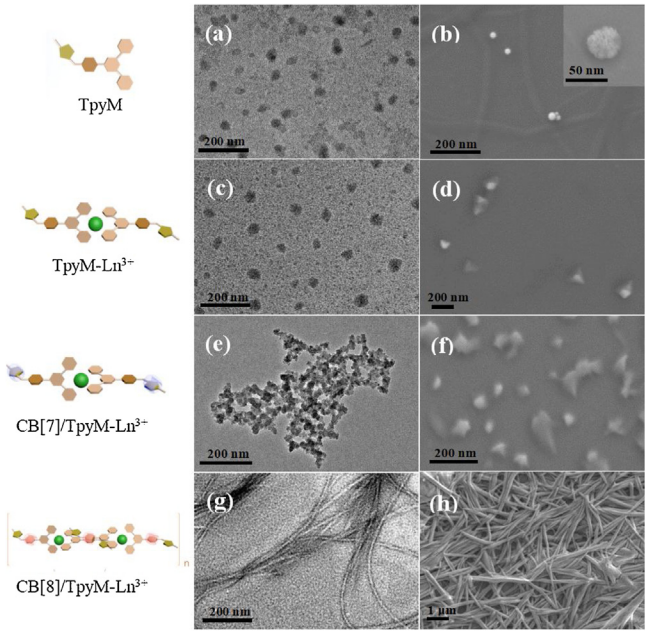

Fig. 2. TEM and SEM images of TpyM (a, b), TpyM-Ln^{3+} (c, d), CB[7]/TpyM-Ln^{3+} (e, f), CB[8]/TpyM-Ln^{3+} (g, h) (Ln = Tb).

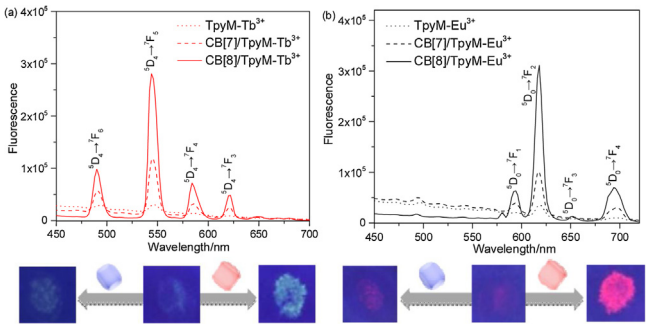

Fig. 3. Solid fluorescence emission spectra and the photos (under 254 nm light) of (a) TpyM-Tb^{3+}, CB[7]/TpyM-Tb^{3+} and CB[8]/TpyM-Tb^{3+}, (b) TpyM-Eu^{3+}, CB[7]/TpyM-Eu^{3+} and CB[8]/TpyM-Eu^{3+} (0.05 mmol/L, λ_{ex} = 290 nm).

compare with those of TpyM-Ln^{3+} and CB[7]/TpyM-Ln^{3+} (Fig. 3). In the control experiment, the fluorescence emission intensity only gave a slight enhancement upon the addition of 2 equiv. of CB[7].

Benefiting from the excellent luminescence properties of Ln^{3+}, CB[8]/TpyM-Ln^{3+} displayed satisfactory luminescence in the solid state. When excited at 290 nm, CB[8]/TpyM-Tb^{3+} showed four sharp emission peaks at 490 nm ($^5D_4 \rightarrow {}^7F_6$), 545 nm ($^5D_4 \rightarrow {}^7F_5$), 585 nm ($^5D_4 \rightarrow {}^7F_4$) and 621 nm ($^5D_4 \rightarrow {}^7F_3$), respectively. The fluorescence of CB[8]/TpyM-Tb^{3+} may be attributed to intramolecular energy transfer (ET) from the excited chelating ligand TpyM to Tb^{3+}. Similar changes in fluorescence spectra were also observed in the case of Eu^{3+}ion. The emission spectra of CB[8]/TpyM-Eu^{3+} exhibited four sharp bands at 594, 618, 652 and 694 nm (Fig. S12 in Supporting information) assigned to the $^5D_0 \rightarrow {}^7F_1$, $^5D_0 \rightarrow {}^7F_2$, $^5D_0 \rightarrow {}^7F_3$ and $^5D_0 \rightarrow {}^7F_4$ transitions of Eu^{3+}, respectively.

To further investigate the relationship between the concentration of CB[8] and the solid fluorescence intensity of supramolecular assembly, solid fluorescence emission spectra of CB[8]/TpyM-Ln^{3+} with the gradually increasing of CB[8] were shown in Fig. S13 in Supporting information. Generally, the solid fluorescence intensity of CB[8]/TpyM-Ln^{3+} increased with the increase of CB[8] concentration. When CB[8] concentration were 0.01 mmol/L, the solid fluorescence intensity all reached to the maximum. Accordingly, the fluorescence lifetime (quantum yield) of CB[8]/TpyM-Tb^{3+} and CB[8]/TpyM-Eu^{3+} assemblies were detected as 0.90 ms (10.3%) and 0.58 ms (11.0%), respectively (Fig. S16 in Supporting information, Table 1), which were larger than those of TpyM-Ln^{3+} and CB[7]/TpyM-Ln^{3+}. Besides, as the increasing of excitation wavelengths from 290 nm to 370 nm, the solid fluorescence emission of CB[8]/TpyM-Tb^{3+} and CB[8]/TpyM-Eu^{3+} all quenched gradually (Fig. S14 in Supporting information). These jointly demonstrated that the lanthanide luminescence intensity of supramolecular assembly could be regulated by CB[8]. In addition, we also measured the solid fluorescence intensities of nanostructures at different times, because the size of nanostructure generally increased with the increasing time of supramolecular assembly. The results showed that no obvious changes of fluorescence intensities of nanofibers or nanoparticles at different times were observed (Fig. S17 in Supporting information). We thus assumed that the fluorescence

Table 1
Luminescence quantum efficiency (Φ) and lifetimes (τ) of various samples.

Sample	Φ (%)	τ_1 (ms)	τ_2 (ms)	χ^2
TpyM-Tb^{3+}	3.2	0.22 (15.20%)	0.90 (84.80%)	1.239
CB[7]/TpyM-Tb^{3+}	5.7	0.34 (21.33%)	1.04 (78.67%)	1.353
CB[8]/TpyM-Tb^{3+}	10.3	0.44 (15.34%)	0.98 (84.66%)	1.199
TpyM-Eu^{3+}	5.6	0.32 (66.78%)	0.77 (33.22%)	0.957
CB[7]/TpyM-Eu^{3+}	6.9	0.29 (65.32%)	0.85 (34.68%)	1.063
CB[8]/TpyM-Eu^{3+}	11.0	0.37 (60.14%)	0.89 (39.86%)	1.231

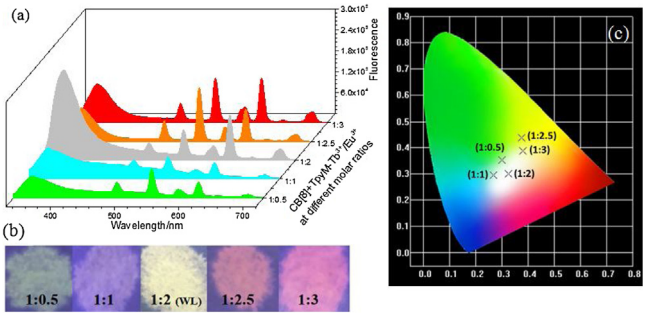

Fig. 4. (a) Solid fluorescence emission spectra and (b) corresponding photos (under 254 nm light) of CB[8]/TpyM-Tb^{3+}/Eu^{3+} at different molar ratios 1:0.5 (0.30, 0.35), 1:1 (0.27, 0.30), 1:2 (0.32, 0.30), 1:2.5 (0.37, 0.44), 1:3 (0.38, 0.39) (λ_{ex} = 290 nm). (c) The 1931 CIE diagram showing the points of color changes based on the fluorescence emission spectra.

intensity may not be related to the length of nanofibers or the diameter of nanoparticles.

Compared with single-color-emissive materials, white-light luminescent materials offer the more potential for their multi-spectrum chromism. We therefore specifically focused on characterizing the white-light emissive properties of CB[8]/TpyM-Ln^{3+} assembly in the solid state. Because the solid state emissions of CB[8]/TpyM-Ln^{3+} contained blue, green and red colors when excited at 254 nm, the entire visible spectrum (400-800 nm) could be covered *via* an RGB (red, green and blue) approach. When Tb^{3+} and Eu^{3+} ions at different molar ratios were simultaneously added into a mixture of CB[8]/TpyM, a series of polymetallic CB[8]/TpyM-Ln^{3+} assemblies could be achieved, showing strong green, cyan, white, orange and red fluorescence (Fig. 4b). Moreover, the corresponding emission spectrum of CB[8]/TpyM-Ln^{3+} could be analyzed as a combination of characteristic emissions of Tb^{3+} (490 and 545 nm) and Eu^{3+} (594, 618, 652 and 694 nm) (Fig. 4a). The 1931 CIE diagram showed the points of the solid fluorescence emission of CB[8]/TpyM-Tb^{3+}, CB[8]/TpyM-Eu^{3+} with different molar ratios of 1:0.5 (0.30, 0.35), 1:1 (0.27, 0.30), 1:2 (0.32, 0.30), 1:2.5 (0.37, 0.44), 1:3 (0.38, 0.39) under 290 nm UV light. Importantly, when the ratio of CB[8]/TpyM-Tb^{3+} *vs.* CB[8]/TpyM-Eu^{3+} reached 1:2, the clear white light emission with a CIE coordinate of (0.32, 0.30) could be observed (Fig. 4c) even when varying the excitation wavelength from 250 to 330 nm (Fig. S15 in Supporting information).

In summary, a wire-like supramolecular assembly based on terpyridine/lanthanide complexes as fluorophores and cucurbit[8]urils as connectors was successfully constructed. Significantly, this supramolecular assembly possessed a CB[8]-induced enhancement of solid state fluorophore, probably because of the unique 1:2 binding of CB[8] cavity towards the cationic guests and the formation of ordered fibrous supramolecular system. By smartly adjusting the ratio of rare earth ions, multi-color lanthanide luminescence, especially white light, were obtained. We do believe that the wire-like supramolecular assembly with a convenient approach and tunable enhanced lanthanide luminescence would become one of the most promising smart lanthanide luminescent materials.

Acknowledgment

We thank the National Natural Science Foundation of China (Nos. 21672113, 21432004, 21772099, 21861132001 and 91527301) for financial support.

Appendix A. Supplementary data

Supplementary material related to this article can be found, in the online version, at doi:https://doi.org/10.1016/j.cclet.2018.12.029.

References

[1] Y. Zhou, H.Y. Zhang, Z.Y. Zhang, Y. Liu, J. Am. Chem. Soc. 139 (2017) 7168–7171.
[2] L. Li, C.K. Tsung, Z. Yang, et al., Adv. Mater. 20 (2008) 903–908.
[3] M.M. Lezhnina, T. Jüstel, H. Kätker, D.U. Wiechert, U.H. Kynast, Adv. Funct. Mater. 16 (2006) 935–942.
[4] J. Thompson, R.I.R. Blyth, G. Gigli, R. Cingolani, Adv. Funct. Mater. 14 (2004) 979–984.
[5] J.C.G. Bünzli, Chem. Rev. 110 (2010) 2729–2755.
[6] S.S. Babu, V.K. Praveen, A. Ajayaghosh, Chem. Rev. 114 (2014) 1973–2129.
[7] Y. Sagara, T. Kato, Nat. Chem. 1 (2009) 605–610.
[8] X.M. Chen, Y. Chen, L. Liang, Q.J. Liu, Y. Liu, Macromol. Rapid Commun. 39 (2018)1700869.
[9] X.L. Ni, S. Chen, Y. Yang, Z. Tao, J. Am. Chem. Soc. 138 (2016) 6177–6183.
[10] Q. Zhao, Y. Chen, S.H. Li, Y. Liu, Chem. Commun. 54 (2018) 200–203.
[11] J. Lagona, P. Mukhopadhyay, S. Chakrabarti, L. Isaacs, Angew. Chem. Int. Ed. 44 (2005) 4844–4870.
[12] E. Masson, X. Ling, R. Joseph, L. Kyeremeh-Mensah, X. Lu, RSC Adv. 2 (2012) 1213–1247.
[13] Y. Zhang, Y. Chen, J. Li, L. Liang, Y. Liu, Acta Chim. Sinica 76 (2018) 622–626.
[14] Q. Zhao, Y. Chen, Y. Liu, Chin. Chem. Lett. 29 (2018) 84–86.
[15] Y. Chen, F. Huang, Z.T. Li, Y. Liu, Sci. China Chem. 61 (2018) 979–992.
[16] Y.H. Ko, E. Kim, I. Hwang, K. Kim, Chem. Commun. (2007) 1305–1315.
[17] S. Gurbuz, M. Idris, D. Tuncel, Org. Biomol. Chem. 13 (2015) 330–347.
[18] A. Appel Eric, J. Dyson, J. Barrio, Z. Walsh, A. Scherman Oren, Angew. Chem. Int. Ed. 51 (2012) 4185–4189.
[19] Y. Lan, X.J. Loh, J. Geng, Z. Walsh, O.A. Scherman, Chem. Commun. 48 (2012) 8757–8759.
[20] S.D. Choudhury, N. Barooah, V.K. Aswal, et al., Soft Matter 10 (2014) 3485–3493.
[21] X.J. Loh, J. del Barrio, P.P.C. Toh, et al., Biomacromolecules 13 (2012) 84–91.
[22] Y. Wang, D. Li, H. Wang, et al., Chem. Commun. 50 (2014) 9390–9392.
[23] D. Jiao, J. Geng, J. Loh Xian, et al., Angew. Chem. Int. Ed. 51 (2012) 9633–9637.
[24] X.J. Loh, J. del Barrio, T.C. Lee, O.A. Scherman, Chem. Commun. 50 (2014) 3033–3035.
[25] G. Stephenson, R.M. Parker, Y. Lan, et al., Chem. Commun. 50 (2014) 7048–7051.
[26] F. Tian, N. Cheng, N. Nouvel, J. Geng, O.A. Scherman, Langmuir 26 (2010) 5323–5328.
[27] F. Tian, D. Jiao, F. Biedermann, O.A. Scherman, Nat. Commun. 3 (2012) 1207.
[28] K.D. Zhang, J. Tian, D. Hanifi, et al., J. Am. Chem. Soc. 135 (2013) 17913–17918.
[29] E.A. Appel, F. Biedermann, U. Rauwald, et al., J. Am. Chem. Soc. 132 (2010) 14251–14260.
[30] R. Joseph, A. Nkrumah, R.J. Clark, E. Masson, J. Am. Chem. Soc. 136 (2014) 6602–6607.
[31] M. Raeisi, K. Kotturi, I. del Valle, et al., J. Am. Chem. Soc. 140 (2018) 3371–3377.
[32] O. Kotova, R. Daly, M.G. Cidália, et al., Angew. Chem. Int. Ed. 51 (2012) 7208–7212.
[33] P. Chen, Q. Li, S. Grindy, N. Holten-Andersen, J. Am. Chem. Soc. 137 (2015) 11590–11593.
[34] S.V. Eliseeva, J.C.G. Bunzli, Chem. Soc. Rev. 39 (2010) 189–227.
[35] J.C.G. Bunzli, C. Piguet, Chem. Soc. Rev. 34 (2005) 1048–1077.
[36] A. Tigaa Rodney, X. Aerken, A. Fuchs, A. de Bettencourt-Dias, Eur. J. Inorg. Chem. 2017 (2017) 5310–5317.
[37] J. Liu, Y. Tan Cindy Soo, Z. Yu, et al., Adv. Mater. 29 (2017)1605325.